Subsections

3.2 Phase plane analysis

In two-dimensional models, the temporal evolution of the variables $(u, w)^T$ can be visualized in the so-called phase plane. From a starting point $(u(t), w(t))^T$ the system will move in a time Δt to a new state $(u(t+\Delta t), w(t+\Delta t))^T$ which has to be determined by integration of the differential equations (3.2) and (3.3). For Δt sufficiently small, the displacement $(\Delta u, \Delta w)^T$ is in the direction of the flow $(\dot{u}, \dot{w})^T$, i.e.,

$$\begin{pmatrix} \Delta u \\ \Delta w \end{pmatrix} = \begin{pmatrix} \dot{u} \\ \dot{w} \end{pmatrix} \Delta t\,, \tag{3.22}$$

which can be plotted as a vector field in the phase plane. Here $\dot{u} = \mathrm{d}u/\mathrm{d}t$ is given by (3.2) and $\dot{w} = \mathrm{d}w/\mathrm{d}t$ by (3.3). The flow field is also called the phase portrait of the system. An important tool in the construction of the phase portrait are the nullclines which are introduced now.

3.2.1 Nullclines

Let us consider the set of points with $\dot{u} = 0$, called the *u*-nullcline. The direction of flow on the *u*-nullcline is in direction of $(0, \dot{w})^T$, since $\dot{u} = 0$. Hence arrows in the phase portrait are vertical on the *u*-nullcline. Similarly, the *w*-nullcline is defined by the condition $\dot{w} = 0$ and arrows are horizontal. The fixed points of the dynamics, defined by $\dot{u} = \dot{w} = 0$ are given by the intersection of the *u*-nullcline with the *w*-nullcline. In Fig. 3.2 we have three fixed points.

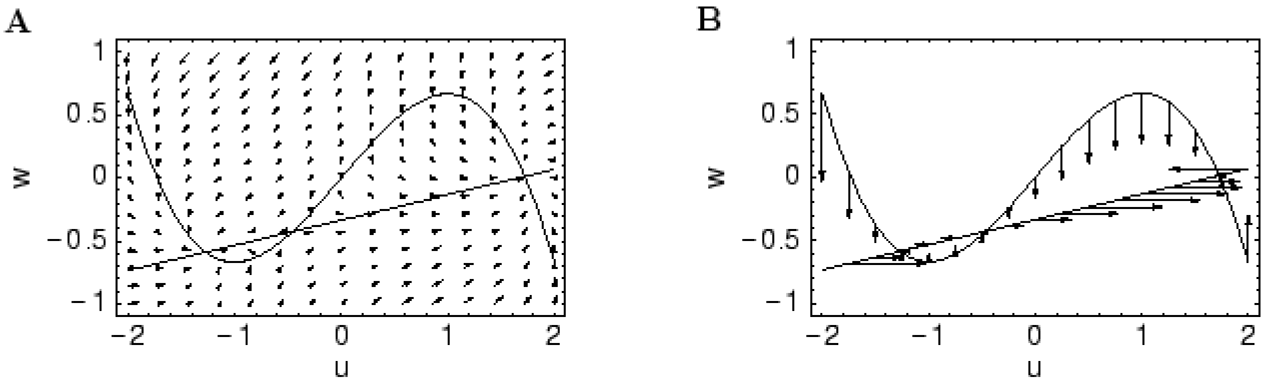

Figure 3.2: **A**. Phase portrait of the FitzHugh-Nagumo model. The *u*-nullcline (curved line) and the *w*-nullcline (straight line) intersect at the three fixed points. The direction of the arrows indicates the flow $(\dot{u}, \dot{w})^T$. **B**. Arrows on the *u*-nullcline point vertically upward or downward, on the *w* nullcline arrows are horizontal. In the neighborhood of the fixed points arrows have short length indicating slow movement. At the fixed point, the direction of arrows changes.

So far we have argued that arrows on the *u*-nullcline are vertical, but we do not know yet whether they point up or down. To get the extra information needed, let us return to the *w*-nullcline. By definition, it separates the region with $\dot{w} > 0$ from the area with $\dot{w} < 0$. Suppose we evaluate $G(u, w)$ on the right-hand side of Eq. (3.3) at a single point, e.g, at (0, 1). If $G(0, 1) > 0$, then the whole area on that side of the *w*-nullcline has $\dot{w} > 0$. Hence, all arrows along the *u*-nullcline that lie on the same side of the *w*-nullcline as the point (0, 1) point upwards. The direction of arrows normally[3.1] changes where the nullclines intersect; cf. Fig. 3.2B.

3.2.2 Stability of Fixed Points

In Fig. 3.2 there are three fixed points, but which of these are stable? The local stability of a fixed point (u_{FP}, w_{FP}) is determined by linearization of the dynamics at the intersection. With $\vec{x} = (u - u_{FP}, w - w_{FP})^T$, we have after the linearization

$$\frac{\mathrm{d}}{\mathrm{d}t}\vec{x} = \begin{pmatrix} F_u & F_w \\ G_u & G_w \end{pmatrix} \vec{x} \;, \tag{3.23}$$

where $F_u = \partial F/\partial u$, $F_w = \partial F/\partial w$, ..., are evaluated at the fixed point. To study the stability we set $\vec{x}(t) = \vec{e}\,\exp(\lambda t)$ and solve the resulting eigenvalue problem. There are two solutions with eigenvalues λ_+ and λ_- and eigenvectors $\vec{e}_+$ and $\vec{e}_-$, respectively. Stability of the fixed point $\vec{x} = 0$ in Eq. (3.23) requires that the real part of both eigenvalues be negative. The solution of the eigenvalue problem yields $\lambda_+ + \lambda_- = F_u + G_w$ and $\lambda_+ \lambda_- = F_u G_w - F_w G_u$. The necessary and sufficient condition for stability is therefore

$$F_u + G_w < 0 \quad and \quad F_u G_w - F_w G_u > 0 \,. \tag{3.24}$$

If $F_u G_w - F_w G_u < 0$, then the imaginary part of both eigenvalues vanishes. One of the eigenvalues is positive, the other one negative. The fixed point is then called a saddle point.

Eq. (3.23) is obtained by Taylor expansion of Eqs. (3.2) and (3.3) to first order in $\vec{x}$. If the real part of one or both eigenvalues of the matrix in Eq. (3.23) vanishes, the complete characterization of the stability properties of the fixed point requires an extension of the Taylor expansion to higher order.

3.2.2.1 Example: Linear model

Let us consider the linear dynamics

$$\dot{u} = a\,u - w$$
$$\dot{w} = \epsilon\,(b\,u - w)\,, \tag{3.25}$$

with positive constants $b, \epsilon > 0$. The u-nullcline is $w = a\,u$, the w-nullcline is $w = b\,u$. For the moment we assume $a < 0$. The phase diagram is that of Fig. 3.3A. Note that by decreasing the parameter ϵ, we may slow down the w-dynamics in Eq. (3.25) without changing the nullclines.

Because of $F_u + G_w = a - \epsilon < 0$ for $a < 0$ and $F_u G_w - F_w G_u = \epsilon\,(b - a) > 0$, it follows from (3.23) that the fixed point is stable. Note that the phase portrait around the left fixed point in Fig. 3.2 has locally the same structure as the portrait in Fig. 3.3A. We conclude that the left fixed point in Fig. 3.2 is stable.

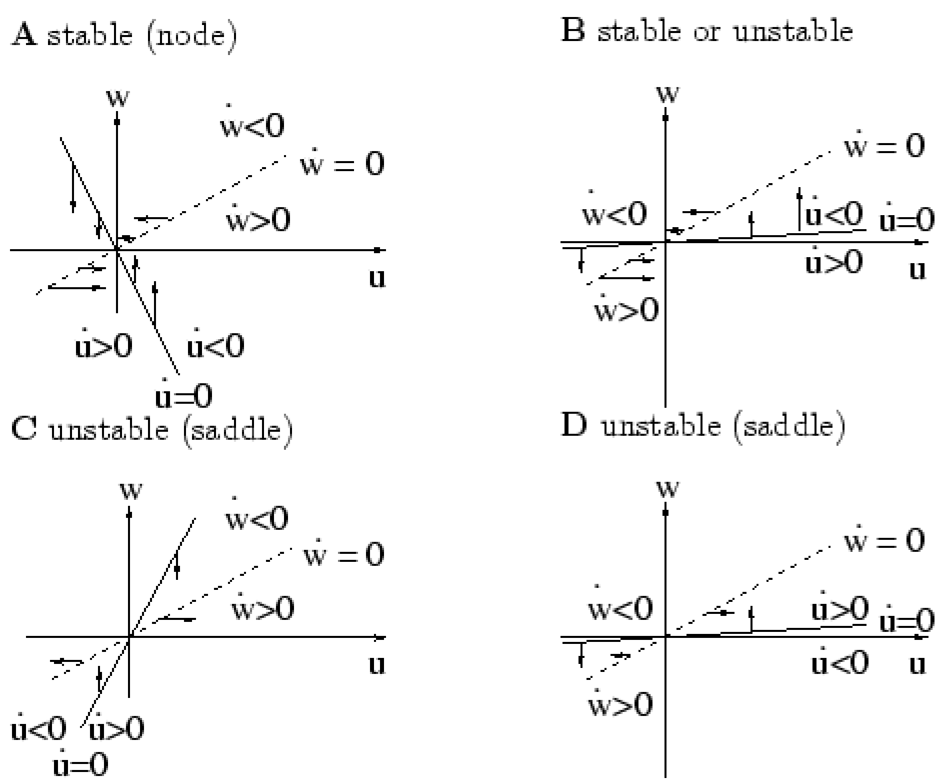

Figure 3.3: Four examples of phase portraits around a fixed point. Case A is stable, case C and D are unstable. Stability in case B cannot be decided with the information available from the picture alone. C and D are saddle points.

Let us now keep the w-nullcline fixed and turn the u-nullcline by increasing a to positive values; cf. Fig. 3.3B and C. Stability is lost if $a > min\{\epsilon, b\}$. Stability of the fixed point in Fig. 3.3B can therefore not be decided without knowing the value of ϵ. On the other hand, in Fig. 3.3C we have $a > b$ and hence $F_u G_w - F_w G_u = \epsilon\,(b - a) < 0$. In this case one of the eigenvalues is positive ($\lambda_+ > 0$) and the other one negative ($\lambda_- < 0$), hence we have a saddle point. The imaginary part of the eigenvalues vanishes. The eigenvectors $\vec{e}_-$ and $\vec{e}_+$ are therefore real and can be visualized in the phase space. A trajectory through the fixed point in direction of $\vec{e}_-$ is attracted towards the fixed point. This is, however, the only direction by which a trajectory may reach the fixed point. Any small perturbation around the fixed point, which is not strictly in direction of $\vec{e}_2$ grows exponentially. A saddle point as in Fig. 3.3C plays an important role in so-called type I neuron models that will be introduced in Section 3.2.4.

For the sake of completeness we also study the linear system

$$\dot{u} = - a\, u + w$$
$$\dot{w} = \epsilon\, (b\, u - w)\ ,\ \text{with } 0 < a < b\ , \tag{3.26}$$

with positive constants a, b, and ϵ. This system is identical to Eq. (3.26) except that the sign of the first equation is flipped. As before we have nullclines $w = a\, u$ and $w = b\, u$; cf. Fig. 3.3D. Note that the nullclines are identical to those in Fig. 3.3B, only the direction of the horizontal arrows on the w-nullcline has changed.

Since $F_u G_w - F_w G_u = \epsilon\, (a - b) < 0$, the fixed point is unstable if $a < b$. In this case, the imaginary part of the eigenvalues vanishes and one of the eigenvalues is positive ($\lambda_+ > 0$) while the other one is negative ($\lambda_- < 0$). This is the definition of a saddle point.

3.2.3 Limit cycles

One of the attractive features of phase plane analysis is that there is a direct method to show the existence of limit cycles. The theorem of Poincaré-Bendixson (Verhulst, 1996; Hale and Koçak, 1991) tells us that, if (i) we can construct a bounding surface around a fixed point so that all flux arrows on the surface are pointing towards the interior, and (ii) the fixed point in the interior is repulsive (real part of both eigenvalues positive), then there must exist a stable limit cycle around that fixed point.

The proof follows from the uniqueness of solutions of differential equations which implies that trajectories cannot cross each other. If all trajectories are pushed away from the fixed point, but cannot leave the bounded surface, then they must finally settle on a limit cycle; cf. Fig. 3.4. Note that this argument holds only in two dimensions.

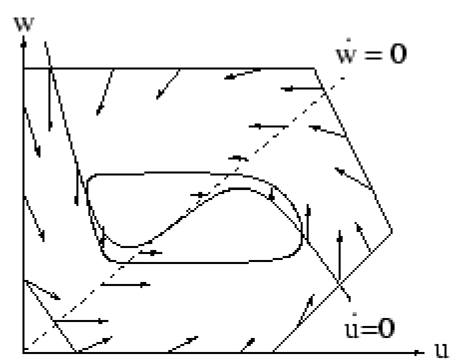

Figure 3.4: Bounding surface around an unstable fixed point and the limit cycle (schematic figure).

3.2.3.1 Example: FitzHugh-Nagumo model

In dimensionless variables the FitzHugh-Nagumo model is

$$\frac{du}{dt} = u - \frac{1}{3} u^3 - w + I \tag{3.27}$$

$$\frac{dw}{dt} = \epsilon \, (b_0 + b_1 \, u - w) \; . \tag{3.28}$$

Time is measured in units of τ and $\epsilon = \tau / \tau_w$ is the ratio of the two time scales. The u-nullcline is $w = u - u^3/3 + I$ with maxima at $u = \pm 1$. The maximal slope of the u-nullcline is $dw/du = 1$ at $u = 0$; for $I = 0$ the u-nullcline has zeros at 0 and $\pm\sqrt{3}$. For $I \neq 0$ the u-nullcline is shifted vertically. The w-nullcline is a straight line $w = b_0 + b_1 \, u$. For $b_1 > 1$, there is always exactly one intersection, whatever I. The two nullclines are shown in Fig. 3.5.

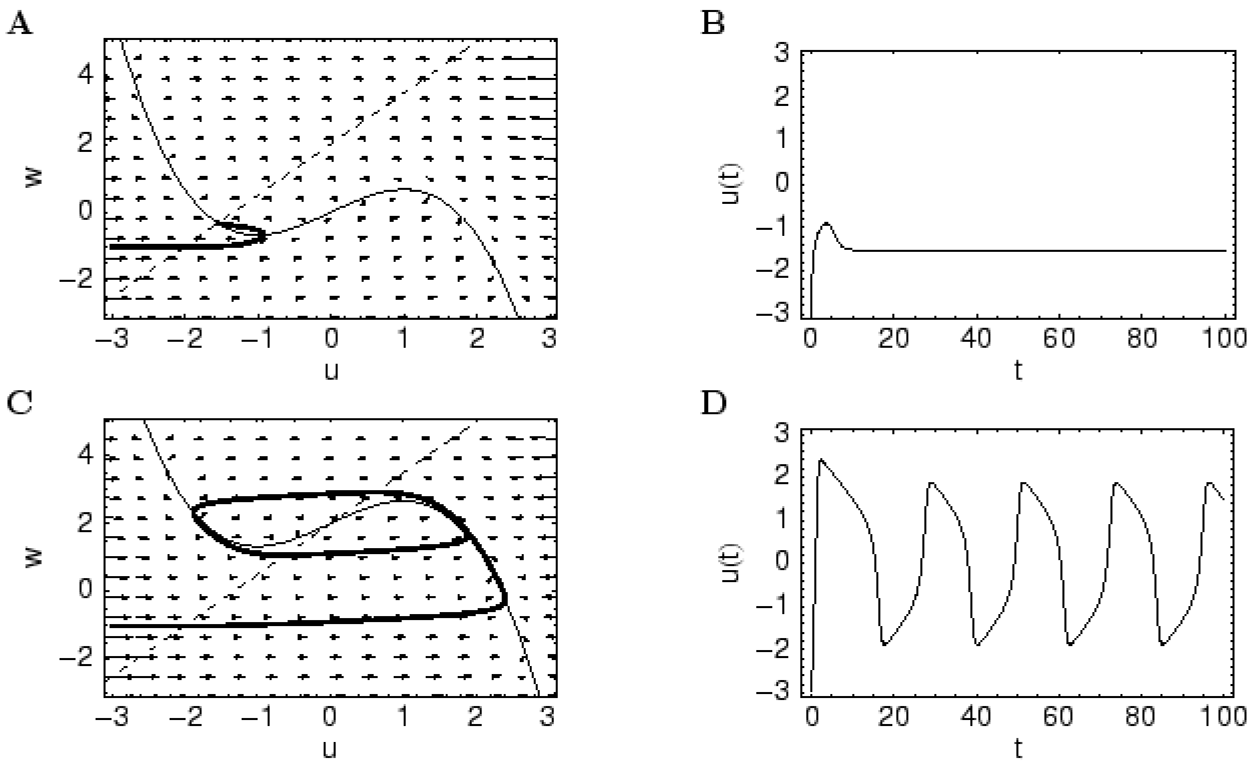

Figure 3.5: **A**. The nullclines of the FitzHugh-Nagumo model for zero input. The thin solid line is the u-nullcline; the w-nullcline is the straight dashed line, $w = b_0 + b_1 u$, with $b_0 = 2$, $b_1 = 1.5$. The fat line is a trajectory that starts at (- 3, - 1) and converges to the fixed point at (- 1.5, - 0.3). **B**. Time course of the membrane potential of the trajectory shown in A. **C**. Same as in A but with positive input $I = 2$ so that the fixed point in A is replaced by a limit cycle (fat line). **D**. Voltage time course of the trajectory shown in C. Trajectories are the result of numerical integration of (3.27) and (3.28) with $\epsilon = 0.1$.

A comparison of Fig. 3.5A with the phase portrait of Fig. 3.3A, shows that the fixed point is stable for $I = 0$. If we increase I the intersection of the nullclines moves to the right; cf. Fig. 3.5C. According to the calculation associated with Fig. 3.3B, the fixed point looses stability as soon as the slope of the u-nullcline becomes larger than ϵ. It is possible to construct a bounding surface around the unstable fixed point so that we know from the Poincaré-Bendixson theorem that a limit cycle must exist. Figures 3.5A and C show two trajectories, one for $I = 0$ converging to the fixed point and another one for $I = 2$ converging towards the limit cycle. The horizontal phases of the limit cycle correspond to a rapid change of the voltage, which results in voltage pulses similar to a train of action potentials; cf. Fig. 3.5D.

3.2.3.2 Hopf bifurcation (*)

We have seen in the previous example that, while I is increased, the behavior of the system changes qualitatively from a stable fixed point to a limit cycle. The point where the transition occurs is called a bifurcation point, and I is the bifurcation parameter. Note that the fixed point $(u(t), w(t)) = (u_{\rm FP}, w_{\rm FP})$ remains a solution of the dynamics whatever the value of I. At some point, however, the fixed point looses its stability, which implies that the real part of at least one of the eigenvalues changes from negative to positive. In other words, the real part passes through zero. From the solution of the stability problem (3.23) we find that at this point, the eigenvalues are

$$\lambda_{\pm} = \pm i\sqrt{F_u G_w - G_u F_w}\ . \tag{3.29}$$

These eigenvalues correspond to an oscillatory solution (of the linearized equation) with a frequency given by $\sqrt{F_u G_w - G_u F_w}$. The above scenario of stability loss in combination with an emerging oscillation is called a Hopf-bifurcation.

Unfortunately, the discussion so far does not tell us anything about the stability of the oscillatory solution. If the new oscillatory solution, which appears at the Hopf bifurcation, is itself unstable (which is more difficult to show), the scenario is called a subcritical Hopf-bifurcation. This is the case in the FitzHugh-Nagumo model where due to the instability of the oscillatory solution in the neighborhood of the Hopf bifurcation the dynamics blows up and approaches another limit cycle of large amplitude; cf. Fig. 3.5. The stable large-amplitude limit cycle solution exists in fact already slightly before I reaches the critical value of the Hopf bifurcation. Thus there is a small regime of bistability between the fixed point and the limit cycle.

In a supercritical Hopf bifurcation, on the other hand, the new periodic solution is stable. In this case, the limit cycle would have a small amplitude if I is just above the bifurcation point. The amplitude of the oscillation grows with the stimulation I.

Whenever we have a Hopf bifurcation, be it subcritical or supercritical, the limit cycle starts with finite frequency. Thus if we plot the frequency of the oscillation in the limit cycle as a function of the (constant) input I, we find a discontinuity at the bifurcation point. Models where the onset of oscillations occurs with nonzero frequency are called type II excitable membrane models. Type I models have an onset of oscillations with zero frequency as will be discussed in the next subsection.

3.2.4 Type I and type II models

In the previous example, there was exactly one fixed point whatever I. If I is slowly increased, the neuronal dynamics changes from stationary to oscillatory at a critical value of I where the fixed point changes from stable to unstable via a (subcritical) Hopf bifurcation. In this case, the onset occurs with nonzero frequency and the model is classified as type II.

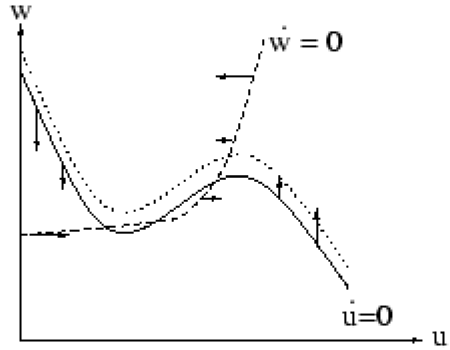

Figure 3.6: The nullclines of a type I model. For zero input, the *u*-nullcline (solid line) has three intersections with the *w*-nullcline (dashed). For input $I > 0$, the *u*-nullcline is shifted vertically (dotted line) and, if I is sufficiently large, only one fixed point remains which is unstable.

A different situation is shown in Fig. 3.6. For zero input, there are three fixed points: A stable fixed point to the left, a saddle point in the middle, and an unstable fixed point to the right. If I is increased, the u-nullcline moves upwards and the stable fixed point merges with the saddle and disappears. We are left with the unstable fixed point around which there must be a limit cycle provided the flux is bounded. At the transition point the limit cycle has zero frequency because it passes through the two merging fixed points where the velocity of the trajectory is zero. If I is increased a little, the limit cycle still `feels' the disappeared fixed points in the sense that the velocity of the trajectory in that region is very low. Thus the onset of oscillation is continuous and occurs with zero frequency. Models which fall into this class are called type I; cf. Fig. 3.7.

From the above discussion it should be clear that, if we increase I, we encounter a transition point where two fixed points disappear, viz., the saddle and the stable fixed point (node). At the same time a limit cycle appears. If we come from the other side, we have first a limit cycle which disappears at the moment when the saddle-node pair shows up. The transition is therefore called a saddle-node bifurcation on a limit cycle.

3.2.4.1 Example: FitzHugh-Nagumo model

The appearance of oscillations in the FitzHugh-Nagumo Model discussed above is of type II. If the slope of the w-nullcline is larger than one, there is only one fixed point, whatever I. This fixed point looses stability via a Hopf bifurcation.

On the other hand, if the slope of the w-nullcline is smaller than one, it is possible to have three fixed points, one of them unstable the other two stable; cf. Fig. 3.2. The system is then bistable and no oscillation occurs.

3.2.4.2 Example: Morris-Lecar model

Depending on the choice of parameters, the Morris-Lecar model is of either type I or type II. In contrast to the FitzHugh-Nagumo model the w-nullcline is not a straight line but has positive curvature. It is therefore possible to have three fixed points so that two of them lie in the unstable region where u has large positive slope as indicated schematically in Fig. 3.6. Comparison of the phase portrait of Fig. 3.6 with that of Fig. 3.3 shows that the left fixed point is stable as in Fig. 3.3A, the middle one is a saddle point as in Fig. 3.3C, and the right one is unstable as in Fig. 3.3B provided that the slope of the u-nullcline is sufficiently positive. Thus we have the sequence of three fixed points necessary for a type I model.

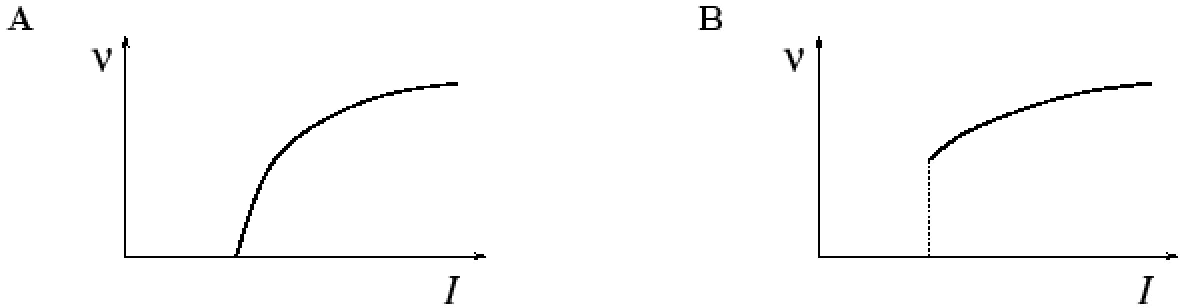

Figure 3.7: **A**. Gain function for models of type I. The frequency ν during a limit cycle oscillation is a continuous function of the applied current *I*. **B**. The gain function of type II models has a discontinuity.

3.2.4.3 Example: Canonical type I model

Consider the one-dimensional model

$$\frac{\mathrm{d}\phi}{\mathrm{d}t} = q\,(1 - \cos\phi) + I\,(1 + \cos\phi) \tag{3.30}$$

where $q > 0$ is a parameter and I with $0 < |I| < q$ the applied current. The variable ϕ is the phase along the limit cycle trajectory. For all currents $I > 0$, we have $\mathrm{d}\phi/\mathrm{d}t > 0$, so that the system is circling along the limit cycle. The minimal velocity is $\mathrm{d}\phi/\mathrm{d}t = I$ for $\phi = 0$. Formally, a spike is said to occur whenever $\phi = \pi$. The period of the limit cycle can be found by integration of (3.30) around a full cycle.

Let us now reduce the amplitude of the applied current *I*. For $I \rightarrow 0$, the velocity along the trajectory around $\phi = 0$ tends to zero. The period of one cycle $T(I)$ therefore tends to infinity. In other words, for $I \rightarrow 0$, the frequency of the oscillation $\nu = 1/T(I)$ decreases (continuously) to zero. For $I < 0$, Eq. (3.30) has a stable fixed point at $\phi = 0$; see Fig. 3.8.

The model (3.30) is a canonical model in the sense that all type I neuron models close to the bifurcation point can be mapped onto (3.30) (Ermentrout, 1996).

A B

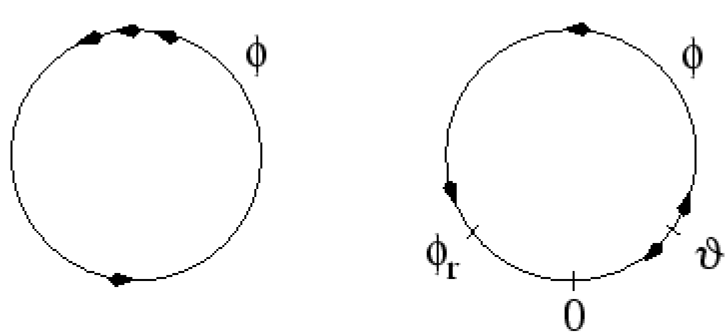

Figure 3.8: Type I model as a phase model. **A**. For $I >$ 0, the system is on a limit cycle. The phase velocity $\mathrm{d}\phi$ $/\mathrm{d}t$ is everywhere positive. **B**. For $I < 0$, the phase has a

stable fixed point at $\phi = \phi_r$ and an unstable fixed point at $\phi = \vartheta$.

Next: 3.3 Threshold and excitability **Up:** 3. Two-Dimensional Neuron Models **Previous:** 3.1 Reduction to two

Gerstner and Kistler
Spiking Neuron Models. Single Neurons, Populations, Plasticity
Cambridge University Press, 2002